DOI: 10.1002/cbic.201000125

Multivalent Display and Receptor-Mediated Endocytosis of Transferrin on Virus-Like Particles

Deboshri Banerjee,[a] Allen P. Liu,[b] Neil R. Voss,[b] Sandra L. Schmid,*[b] and M. G. Finn*[a]

The structurally regular and stable self-assembled capsids derived from viruses can be used as scaffolds for the display of multiple copies of cell- and tissue-targeting molecules and therapeutic agents in a convenient and well-defined manner. The human iron-transfer protein transferrin, a high affinity ligand for receptors upregulated in a variety of cancers, has been arrayed on the exterior surface of the protein capsid of bacteriophage Qβ. Selective oxidation of the sialic acid residues on the glycan chains of transferrin was followed by introduction of a terminal alkyne functionality through an oxime linkage. Attachment of the protein to azide-functionalized Qβ capsid particles in an orientation allowing access to the receptor binding site was accomplished by the Cu^{I}-catalyzed azide–alkyne cycloaddition (CuAAC) click reaction. Transferrin conjugation to Qβ particles allowed specific recognition by transferrin receptors and cellular internalization through clathrin-mediated endocytosis, as determined by fluorescence microscopy on cells expressing GFP-labeled clathrin light chains. By testing Qβ particles bearing different numbers of transferrin molecules, it was demonstrated that cellular uptake was proportional to ligand density, but that internalization was inhibited by equivalent concentrations of free transferrin. These results suggest that cell targeting with transferrin can be improved by local concentration (avidity) effects.

Introduction

Human holo-transferrin (Tfn) is an 80 kDa bi-lobed iron-carrier glycoprotein in vertebrates[1] that is essential for iron homeostasis.[2] Transferrin is specifically recognized by Tfn receptors (TfnR) overexpressed on the surface of a variety of tumor cells[3] and efficiently taken up by cells in a well-characterized process of clathrin-mediated endocytosis.[4] The Tfn–TfnR interaction has been exploited as a potential pathway for uptake of Tfn-conjugated drugs by targeted cells.[4–5] For example, polyvalent assembly of transferrin on liposomes[6] and gold nanoparticles[7] has been reported previously. In the current study, we wished to explore the mechanisms of interactions of TfnR-bearing cells with Tfn displayed on a uniform protein nanoparticle scaffold on which different densities of Tfn could be displayed.

We have previously described the conjugation of transferrin to cowpea mosaic virus (CPMV) by modification of both proteins with complementary azide and alkyne residues, and their subsequent ligation by the efficient Cu^{I}-catalyzed azide–alkyne cycloaddition (CuAAC) "click" reaction.[8] In this study, we used the capsid of bacteriophage Qβ, a virus-like particle (VLP) of 30 nm diameter and icosahedral symmetry, as the scaffold. Qβ consists of 180 copies of a single coat-protein subunit, and, like CPMV,[9] may be chemically addressed by acylation of surface lysine groups.[10] It differs from CPMV in having a higher density of such amine attachment points and an overall smoother structure.

In addition to amine acylation, site-specific modification of proteins such as transferrin is often achieved by selective derivatization of cysteine thiols with maleimide or related electrophilic reagents, or oxidation of N-terminal serine or threonine to corresponding aldehydes and subsequent coupling with alkoxyamines or hydrazine derivatives.[11] A disadvantage of these strategies is the possibility of irreversibly altering the structure or blocking the action of a key region of the protein, such as a catalytic site or binding motif, which may lead to a loss of activity. We describe here the alternative manipulation of transferrin by the derivatization of its sialic acid moieties; this preserves the protein in its functional form and allows us to efficiently and controllably graft it to the surface of the VLP scaffold.

Results and Discussion

Preparation and characterization of Qβ-Tfn conjugates

Use of CuAAC chemistry for the attachment of transferrin to Qβ requires the introduction of an azide or alkyne group to each partner. In a previous study, a maleimide-alkyne linker was used to derivatize transferrin at one or more accessible cysteine residues.[8] While the target cysteines are not supposed to be near the site bound by the transferrin receptor,

[a] Dr. D. Banerjee, Prof. M. G. Finn
Department of Chemistry, The Scripps Research Institute
10550 N. Torrey Pines Road, La Jolla, CA 92037 (USA)
Fax: (+1) 858-784-8850
E-mail: mgfinn@scripps.edu

[b] Dr. A. P. Liu, Dr. N. R. Voss, Prof. S. L. Schmid
Department of Cell Biology, The Scripps Research Institute
10550 N. Torrey Pines Road, La Jolla, CA 92037 (USA)
Fax: (+1) 858-784-9126
E-mail: sandys@scripps.edu

Supporting information for this article is available on the WWW under http://dx.doi.org/10.1002/cbic.201000125.

 © 2010 Wiley-VCH Verlag GmbH & Co. KGaA, Weinheim WILEY InterScience DISCOVER SOMETHING GREAT

their derivatization introduces uncertainty in the position of the attachment site, and therefore in the orientation of the displayed protein. We turned here to the mild periodate oxidation of the sialic acid residues on transferrin. The main form of the human transferrin displays up to four terminal sialic acids per molecule.[12] Desialylated transferrin is reported to be internalized by both asialoglycoprotein and transferrin receptors,[12b,13] and the structure of the Tfn–TfnR interaction shows the glycosylation sites to be on a face of the protein far removed from the receptor-binding site.[14] We therefore anticipated that connections made to derivatized sialic acid should not interfere with receptor-mediated endocytosis.

Oxidation of sialic acids on transferrin was followed by attachment of the aminoether linker **2** through the rapid formation of a physiologically stable oxime linkage;[15] this yielded the alkyne-functionalized transferrin **3** (Scheme 1). In order to determine the extent of this modification on the transferrin structure, a sample was condensed with azide-derivatized fluorescein by using the CuAAC reaction with acceleratory ligand **4** under recently reported optimized conditions.[16] The product was analyzed by SDS-PAGE, which verified covalent attachment of the dye, and by UV–vis spectroscopy. Protein concentration was determined by using the Bradford assay, which showed that an average of 3.4 fluorescein molecules was attached per transferrin (see the Supporting Information). Thus, each transferrin molecule displayed 3–4 oxidized and derivatized sialic acid residues.

The surface-exposed lysine residues of the Qβ capsid were simultaneously derivatized with an alkylazide[8] and AlexaFluor® 568 by reaction with a 35:1 mixture of their corresponding *N*-hydroxysuccinimide esters (Scheme 1). The resulting particles **1** were thereby labeled with a small amount of dye to allow visualization by fluorescence microscopy in cell-binding studies while providing for multiple sites for subsequent transferrin attachment. The yield of **1** after purification of the protein from excess reagent was 80–85%, composed exclusively of intact particles as determined by size-exclusion chromatography (SEC).

Qβ–Tfn conjugates (**5**) were prepared by CuAAC reaction of **1** with **3** in the presence of Cu^{I} and ligand **4**. The conjugates were purified by size-exclusion chromatography (SEC) and characterized by analytical SEC, UV-Vis spectroscopy, dynamic light scattering (DLS), transmission electron microscopy (TEM), SDS-PAGE and Western immunoblotting (Figure 1). The A_{260}/A_{280} ratios confirmed the presence of intact, RNA-containing capsids, and SEC analysis showed **5** to elute more quickly than the underivatized particle; this indicates that the Tfn-decorated particles are larger (Figure 1A). Indeed, TEM showed intact and monodispersed particles of 26 ± 2 nm diameter for the wild-type particles and 29 ± 3 nm for the protein-conjugated particles, determined by automated image analysis. The same trend was observed by DLS, which showed hydrodynamic diameters of 28.4 and 38.4 nm, for underivatized and Tfn-labeled particle **5b**, respectively. Western blot analysis further confirmed the attachment of Tfn molecules to the exterior surface of the virus-like particle (Figure 1D).

The loading of Tfn molecules on the particle surface was determined by densitometry analysis after Coomassie staining of

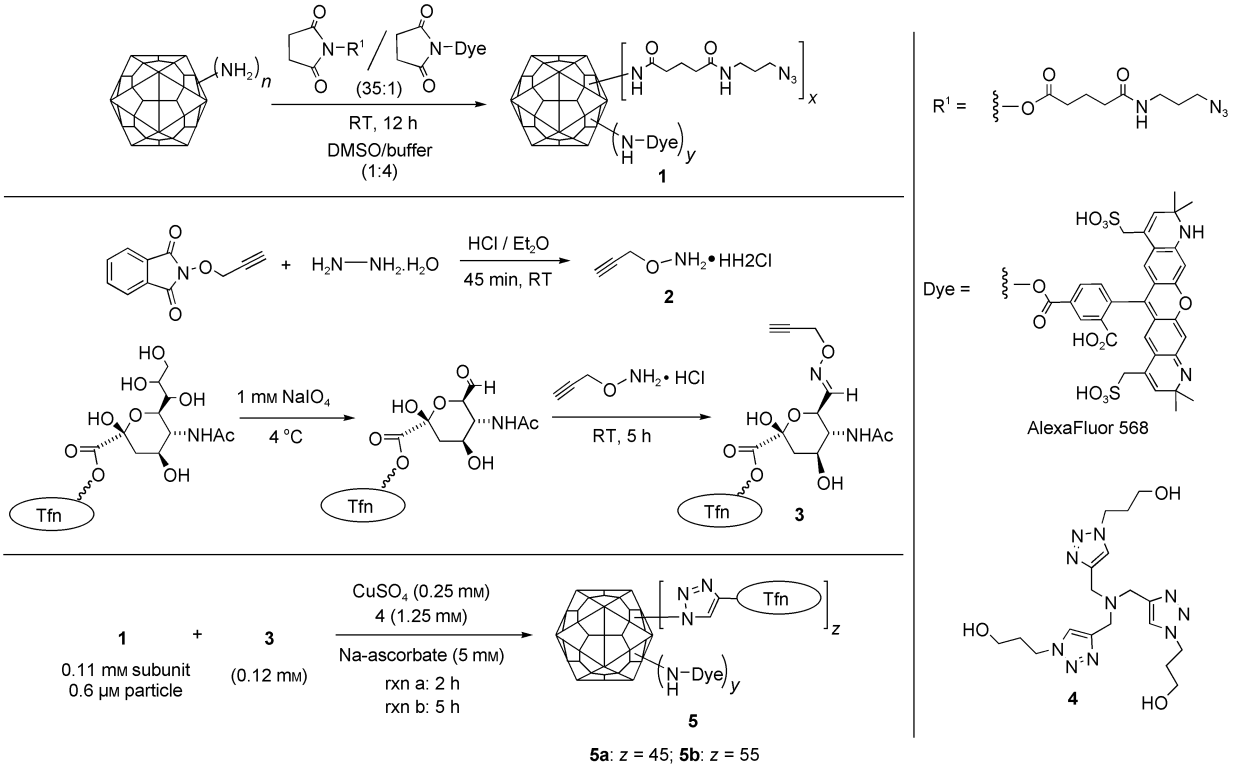

Scheme 1. Synthesis of Qβ-Tfn conjugates.

 © 2010 Wiley-VCH Verlag GmbH & Co. KGaA, Weinheim

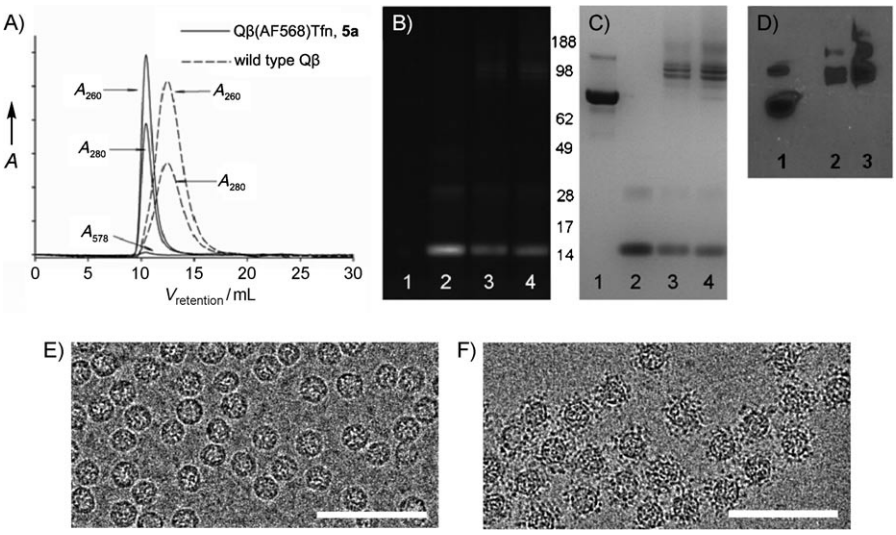

Figure 1. Characterization of Qβ-Tfn conjugates. A) Size-exclusion FPLC (Superose-6 column). B) SDS-PAGE analysis of the protein gel under UV illumination, and C) after SimplyBlue staining. For B) and C), lanes: 1) transferrin, 2) Qβ-azide/dye conjugate **1**, 3) Qβ-Tfn conjugate **5a** (45 Tfn/particle), 4) Qβ-Tfn conjugate **5b** (55 Tfn/particle). D) Western blot analysis, probing with anti-transferrin antibody; lanes: 1) transferrin, 2) **5a**, 3) **5b**. E) TEM of underivatized Qβ. F) TEM of Qβ-Tfn conjugate **5b**. Scale bar = 100 nm.

the SDS-PAGE gel (Figure 1C). Correcting for the relative molecular masses of the components, approximately 45 and 55 transferrin molecules were attached to Qβ VLPs after reaction times of 2 and 5 h, respectively. The CuAAC reaction was therefore revealed to be highly efficient at the micromolar concentrations of azide and alkyne components used, and little improvement was exhibited by longer reaction times.

In an early attempt to make fluorescently labeled particles for cell-binding studies, the red fluorescent protein mCherry was genetically encoded into approximately 15 copies of the Qβ coat protein using a previously published method.[17] While the resulting particles were insufficiently bright for the desired purpose, they were readily addressed with transferrin in analogous fashion to **5b**, resulting in the attachment of approximately 55 Tfn molecules per VLP as before. Cryoelectron microscopy analysis and image reconstruction revealed no difference between the mCherry-containing particles and the wild-type because of the sparse and presumably random distribution of mCherry fusions on the particle surface. In contrast, the cryo-EM image reconstruction of the conjugate of Tfn-alkyne with Qβ(mCherry)-azide (Supporting Information) showed clear density attributable to the added transferrin protein (Figure 2). The bulk of the new density was found approximately 26 Å from the particle surface (shown most clearly in cutaway Figure 2C), consistent with the expected length of the linker connecting the VLP to Tfn.

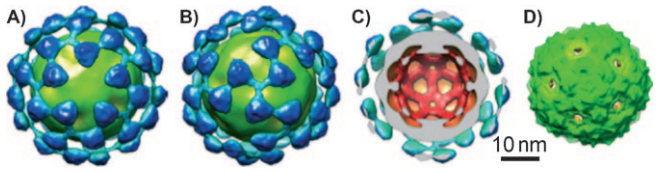

Figure 2. Cryoelectron microscopy image reconstructions at 17.4 Å resolution. A), B) Qβ(mCherry)$(Tfn)_{55}$ conjugate; views down the five- and threefold symmetry axes, respectively. C) Cross-sectional view showing added density other than that of the VLP in light blue. D) Wild-type Qβ and Qβ (mCherry).

Specific binding and internalization of Qβ-Tfn conjugates

Tfn–TfnR complexes are known to enter the cell through clathrin-medicated endoytosis.[18] To monitor clathrin-mediated endocytosis and to study the interaction between Tfn-VLPs and surface-exposed TfnRs, we used African green monkey kidney epithelial cells (BSC1) expressing a fusion between clathrin light chain (Clc) and enhanced green fluorescence protein (EGFP). Similar concentrations of dye-labeled Qβ (**1**) and Qβ-Tfn (**5**) were prebound at 4 °C for 30 min to determine surface binding, and followed by an incubation at 37 °C for 1 h to measure internalization. Surface binding and cellular internalization were analyzed by epifluorescence microscopy of fixed cells (Figure 3). No binding (Figure 3A) or uptake (Figure 3Ai) were observed with **1** even after 60 min at 37 °C; this indicates that Qβ particles neither bind to cell surface receptors nor are internalized by these cells in a nonspecific manner. In contrast, Qβ-Tfn bound to the cell surface at 4 °C (Figure 3Bi) as detected by the red fluorescence of the dye on **5**. Furthermore, substantial internalization was observed after 1 h at 37 °C. The red particles were observed to accumulate in intracellular structures at the cell periphery and in the perinuclear regions indicative of localization in endosomal structures (Figure 3Bii). VLP binding and internalization were abolished in cases in which excess unlabeled free transferrin was included in the incubations (Figure 3Biii); this demonstrated that binding and internalization occur through a Tfn–TfnR mediated pathway.

The involvement of TfnRs during virus uptake was further supported by overexpression of TfnR in BSC1 cells by using adenovirus infection;[19] this resulted in significantly greater binding and uptake of Qβ-Tfn conjugates by the infected cells (and not by the cells in the same sample that escaped adenovirus infection; Figure 3Ci, ii). Binding and internalization of Qβ-Tfn to TfnR overexpressing cells were again abolished in the presence of excess free Tfn (Figure 3Ciii). We also examined the localization of surface bound Qβ-Tfn relative to clathrin-coated pits (CCPs) after 30 min incubation at 4 °C (Figure 3D) and after preincubation followed by 5 min at 37 °C (Supporting Information). Under both conditions, we could identify multiple CCPs containing VLPs; this suggests that CCPs are the transport carrier of VLPs into the cell (Figure 3D, circled spots).

To examine the endocytic mechanism, we performed live cell imaging by total internal reflection fluorescence (TIRF) mi-

 © 2010 Wiley-VCH Verlag GmbH & Co. KGaA, Weinheim

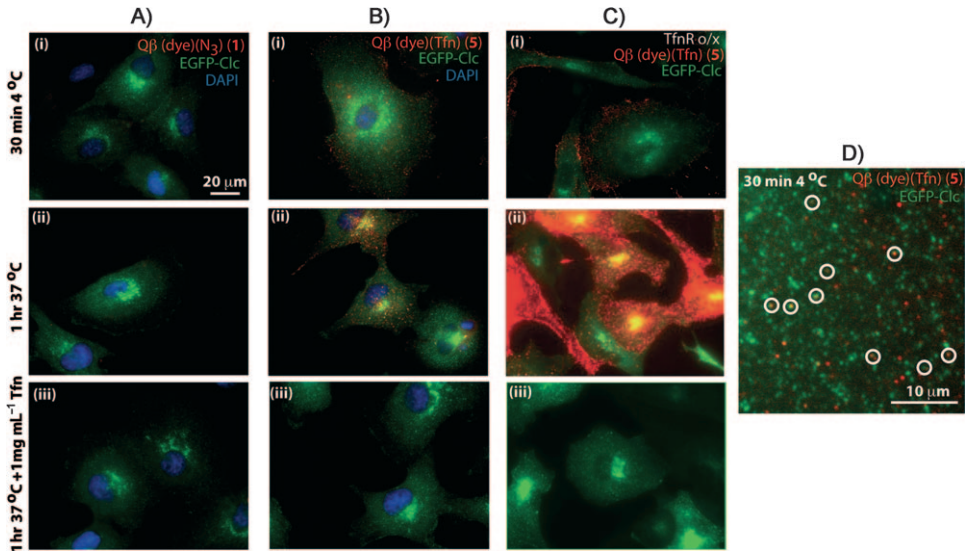

Figure 3. Representative epifluorescence microscopy images showing binding and internalization of VLP particles in EGFP-Clc BSC1 cells. Column A) Qβ particle **1** with EGFP-Clc BSC1 cells. Column B) Qβ-Tfn conjugate **5b** with EGFP-Clc BSC1 cells. Column C) **5b** and EGFP-Clc BSC1 cells overexpressing transferrin receptors. i) After incubation at 4 °C for 30 min. ii) Preincubated at 4 °C followed by shift to 37 °C for 60 min. iii) As in ii) except in the presence of excess free Tfn (1 mg mL^{-1}). D) High-magnification image showing punctate red (**5b**), green (EGFP-Clc), and colocalized (circled) VLPs with CCPs on the surface of a BSC1 cell after 30 min at 4 °C. Very similar images were observed with cells incubated at 37 °C for 5 min (Supporting Information). In all experiments, VLP concentration was 1.2 μg mL^{-1} (0.47 nM in particles).

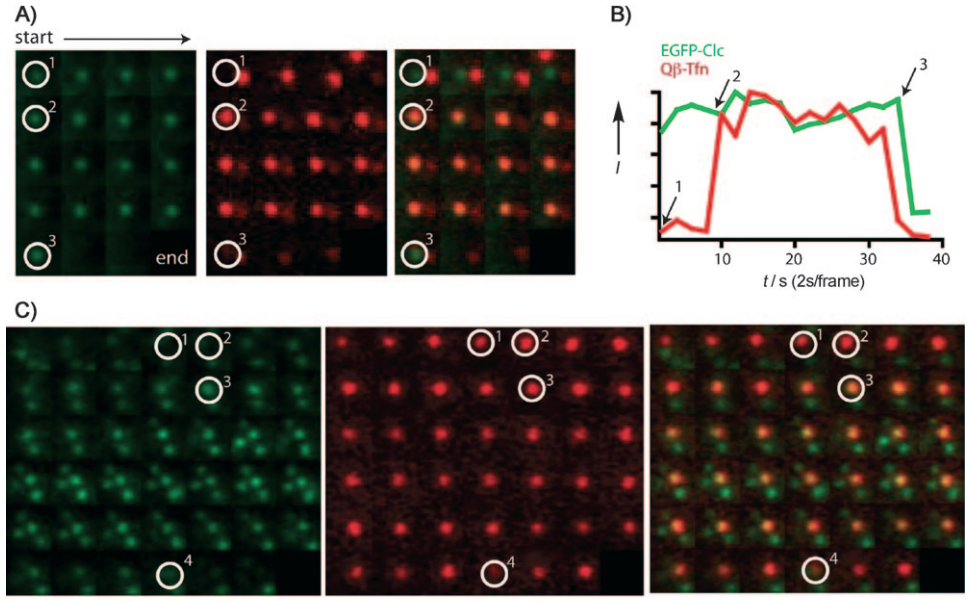

Figure 4. Live cell TIRF images showing green (EGFP-Clc), red (Qβ-Tfn particle **5b**), and merged channels of an approximately 2 μm^2 area of the bottom surface of a BSC1 cell. Images go left-to-right across each row, and from top to bottom, taken at 2 s intervals with the green channel preceding the red channel. A) VLPs associating with a pre-existing coated pit (circled white), followed by internalization of the complex as a whole. Position 1 shows the pre-existing coated pit. Position 2 marks the initial recruitment of the VLP. Position 3 is the time point at which internalization occurs between the acquisition of the green and red channels; note that both are gone at the next time point. B) Plot of intensity profiles of the CCP (green) and VLP (red) at the indicated spot in (A), normalized each to their respective maximum intensity. (C) VLP nucleating a CCP. Position 1 shows a bound VLP but no clathrin signal. At positions marked 2, the CCP is beginning to assemble at the VLP. By position 3, the pit is fully formed, and it is internalized at position 4. In this case the internalized VLP remains close to the plasma membrane, while the clathrin coat disassembles.

croscopy, which selectively illuminates the bottom surface of the plasma membrane (approximately 100 nm penetration depth). Dye-labeled Qβ-Tfn conjugates were added to live cells at 37 °C, and imaged for green fluorescence followed by red at 2 s intervals. Two main dynamic behaviors were observed: the recruitment of surface bound VLP to preformed clathrin-coated pits (CCPs), as shown in Figure 4A and B, and the apparent nucleation of CCPs by VLP binding to the TfnRs (Figure 4C). In both cases, endocytosis was often the result as evidenced by the disappearance or reduced intensity of the red (VLP) and green (clathrin) signals (Figure 4B). These results are reminiscent of those observed for the entry of dengue virus into BSC1 cells by clathrin-mediated endocytosis.[20]

To explore the dependence of internalization on the surface density of transferrin molecules attached to the VLP surface, three versions of AlexaFluor-labeled Qβ-Tfn conjugates were prepared with varying loadings of transferrin per particle, as shown in Scheme 2 and Figure 5. Azide-functionalized VLP **1** was addressed in three different CuAAC reactions, each containing the same total concentration of alkyne but differing in the ratio of transferrin-alkyne and propargyl alcohol. This provides for approximately the same density of triazoles on the particle surface, but differing amounts of the desired protein ligand. Reactions **a** and **b** differed by a factor of 6 in Tfn-alkyne concentration, and resulted in a similar (fivefold) difference in attachment density (five vs. 25 Tfn molecules per capsid). A further sixfold increase in Tfn-alkyne concentration (to 70 μM, reaction **c**) increased the loading of Tfn by only 60 percent (to 40 ± 5 per VLP), presumably because of steric crowding or occlusion of azide sites with increasing density of Tfn molecules on the particle surface. Until such steric limitations were reached at the highest loading, the CuAAC re-

 © 2010 Wiley-VCH Verlag GmbH & Co. KGaA, Weinheim

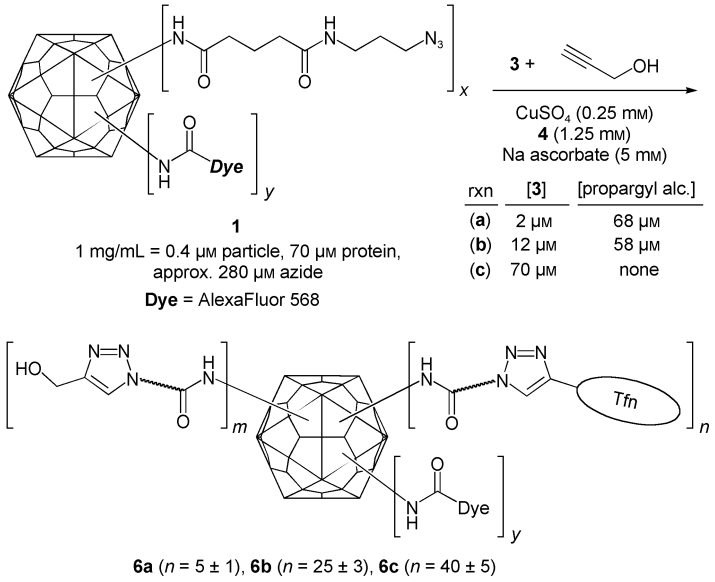

Scheme 2. Synthesis of particles with varying loadings of attached transferrin.

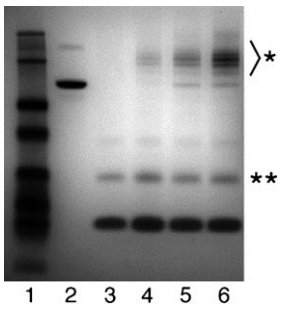

Figure 5. Coomassie stained protein gel of transferrin (lane 2), Qβ-azide **1** (lane 3), Qβ-Tfn conjugates **6a** (lane 4), **6b** (lane 5), and **6c** (lane 6). (Standard protein molecular weight markers appear in lane 1). The bands labeled with a single asterisk denote linked transferrin-Qβ linkages with differing numbers of Qβ coat protein attached to each transferrin molecule. Bands marked with a double asterisk are due to Qβ capsid protein dimers that remain noncovalently associated even under the denaturing conditions of the analysis.

activity of the two alkynes was approximately the same, in spite of their great difference in size (Supporting Information).

The particles **6a–c** were found to be clean, monodisperse structures in the same manner as for conjugates **5**. Dynamic light scattering (DLS) measurements indicated the hydrodynamic diameters of the conjugates to be 32.4, 34.2, and 36.2 nm, respectively, compared to that of 28.4 nm for the wild-type particles and 38.4 nm for particle **5b** bearing the greatest number of Tfn molecules in this study (55 per particle). Mixtures of normal (rather than TfnR-upregulated) BSC1 cells with identical concentrations of dye-labeled Qβ **1** or the three dye-Qβ-Tfn conjugates were analyzed by flow cytometry to allow for more quantitative characterization of the internalization process. Figure 6A and B show results for the negative control **1**, which lacks transferrin, and the particle bearing the greatest density of transferrin ligands, **6c**, respectively. Similar analyses for each of the particles as a function of incubation time with the cells showed maximum internalization to occur within 30–60 min (Figure 6C).

The cellular uptake of Tfn-labeled particles and the inhibition of uptake by free Tfn were found to be consistent with single-point Tfn–TfnR interactions. Thus, while no uptake was observed with dye-labeled Qβ **1** (Figure 6A), significant uptake was seen in a time-dependent manner when cells were incubated with Tfn-labeled VLP (Figure 6B). The extent of uptake was dependent on the number of Tfn units/particle (Figure 6C): only a low amount of specific uptake was observed with **6a**, bearing an average of five Tfn units per particle, uptake was moderate with **6b** (25 Tfn per particle) and quite efficient with **6c** (40 Tfn per particle). Considering the concentrations of Tfn involved (overall ca. 4, 15, and 24 nM for **6a**, **6b**, and **6c**, respectively), these data correspond roughly to what one would expect for a single-point

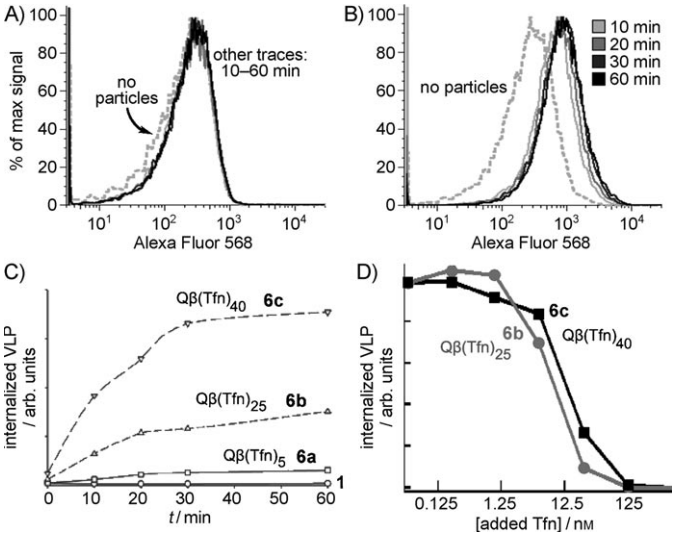

Figure 6. FACS analysis following incubation of Qβ-Tfn conjugates with BSC1 cells at 37 °C for the specified time, followed by washing and chemical fixation. A) Underivatized Qβ VLP 1 (3 μg mL^{-1}, 1.2 nM in particles), showing no evidence of binding. B) Qβ-Tfn VLP 6c (1.6 μg mL^{-1} (0.6 nM in particle), showing significant and rapid virus uptake. C) Summary of data for **1** and **6a–c**, showing that higher Tfn load leads to increased uptake by cells. D) Effect of increasing concentrations of free unlabeled Tfn on cellular uptake of 1.6 μg mL^{-1} **6b** (that is, 0.6 nM particle, 15 nM Tfn) or **6c** (24 nM Tfn) as detected by FACS.

binding interaction of about 5–10 nM; this is consistent with the reported low-nanomolar affinity of Tfn for the Tfn receptor.[21] The efficient internalization of **6b** and **6c** was inhibited with free transferrin in a dose-dependent fashion (Figure 6D), with IC_{50} values of approximately 1 μg mL^{-1} (13 nM) for **6c** and 0.5 μg mL^{-1} (6 nM) for **6b**. For both particles, 10 μg mL^{-1} (125 nM) or more of free transferrin was completely inhibitory, while less than 0.01 μg mL^{-1} (125 pM) had no effect. Because

 © 2010 Wiley-VCH Verlag GmbH & Co. KGaA, Weinheim

Qβ-Tfn uptake was effectively inhibited by approximately equivalent concentrations of free Tfn as were presented by the particles, the Tfn-conjugated VLP ligands did not appear to benefit from their polyvalency with respect to affinity or avidity.

Conclusions

The oxidation and derivatization of the sialic acid residues of transferrin is a convenient and effective method for introducing a connecting linkage that can provide a consistent display geometry while retaining binding affinity to transferrin receptors. Conjugation of transferrin-alkyne thus prepared to the azide-functional groups on the Qβ virus capsid was accomplished using the powerful CuAAC click reaction in a recently reported optimized protocol.[16] These conjugates were specifically internalized by cells expressing transferrin receptors through clathrin-mediated endocytosis.

Our studies represent the first test of transferrin polyvalency on receptor-mediated cell entry in which the protein ligands are arranged in a well-defined platform-based manner. On a per-unit basis, the Qβ-Tfn conjugates have greater affinities for TfnR-bearing cells than free Tfn, and the rates of uptake of Tfn-bearing particles were strongly improved by the attachment of greater numbers of Tfn ligands to each particle (Figure 6C). These findings suggest that polyvalent transferrin conjugates can enhance the targeting of specific cell populations in complex mixtures. However, on a per-Tfn basis, the VLPs did not exhibit significantly increased affinity relative to the free ligand. This interesting disconnection of affinity (or avidity)[22] and internalization efficiency remains unexplained at present, but changes in recycling[23] and intracellular trafficking pathways exhibited by multivalent constructs may be at least partially responsible. These findings make transferrin assemblies potentially useful in the delivery of drugs for therapeutic purposes.[24]

Experimental Section

Details of instrumentation and the purchase or preparation of all reagents, including the Qβ VLPs, are given in the Supporting Information.

Preparation of AlexaFluor 568-labeled Qβ-azide (1): A solution of wild-type Qβ VLPs (5 mg mL^{-1} in 0.1 M phosphate buffer, pH 7) was treated with a premixed DMSO solution of NHS-linker-azide (final concentration 12 mM, 35-fold excess per Qβ subunit) and the NHS ester of the dye (final concentration 0.35 mM), such that the final reaction mixture contained 20% DMSO. The solution was allowed to stand for 12 h at RT, and the derivatized VLP was purified away from excess reagents on a sucrose gradient (10–40%) and concentrated by ultrapelleting. The virus pellet was resuspended in HEPES buffer (0.1 M, pH 7.3). FPLC analysis of **1** indicated that $>95\%$ of the virus consisted of intact particles. Protein concentration was analyzed by using the Coomassie Plus (Bradford) Protein Assay (Pierce).

Synthesis of *O*-(prop-2-ynyl)hydroxylamine (2): Phthalimide-protected *O*-(prop-2-ynyl)hydroxylamine (5.0 g, 24.9 mmol) was stirred with hydrazine monohydrate (1.4 g, 27.8 mmol) for a few minutes before the addition of diethyl ether (25 mL). This mixture was stirred at RT for 45 min. The white precipitate was filtered off and ethereal HCl (18 mL, 2 N) was added to the filtrate with continuous stirring. The yellow-white precipitate was filtered and dried under vacuum to give **2** (2.1 g, 78%), which was characterized by ^{1}H NMR spectroscopy and matched the data previously reported.[25]

Preparation of transferrin-alkyne conjugate (3): Transferrin (2 mg mL^{-1}) was incubated with sodium *meta*-periodate (1 mM) in sodium acetate buffer (0.1 M, pH 5.5; 30 mL) on ice in the dark for 30 min. The mixture was concentrated to less than 1 mL by using centrifugal filter tubes (Millipore), and then dialyzed against HEPES buffer (0.1 M, pH 7.2) using Slide-A-Lyzer Dialysis Cassette Kit (Pierce). The resulting oxidized transferrin was incubated with **5** (8.2 mM, 350-fold excess) in HEPES buffer with DMSO (20%, total volume 25 mL) for 5 h at RT by gentle tumbling. Concentration and dialysis as above provided **3** as a pink solution in HEPES buffer; the protein concentration was estimated by using the Bradford protein assay.

Preparation of Qβ-transferrin conjugate (5) by CuAAC reaction: Two identical reaction mixtures were prepared, each containing Qβ-azide **1** (1.7 mg mL^{-1}, 0.11 mM in protein subunits) and transferrin-alkyne **3** (10.2 mg mL^{-1}, 0.12 mM) in HEPES buffer (0.1 M, pH 7.3, 1 mL), containing sodium ascorbate (5 mM), copper sulfate (0.25 mM) and the ligand **4** (1.25 mM). $CuSO_4$ was mixed with **4** in a separate microtube prior to addition to each reaction mixture. The reaction mixtures were allowed to stand at RT for 2 h and 5 h, respectively. The resulting conjugates (**5a**, **5b**) were purified by size-exclusion FPLC on a Superose 6 column.

For all of the above steps, we used diferric Tfn under conditions designed to minimize the loss of iron. After conjugation, the protein absorbance ratio (A_{465}/A_{280}) was found to be 0.043; this was within the range (0.042–0.046) and indicated the presence of Fe in the protein.[26] If Fe is lost, the ability of the attached Tfn to bind its receptor would be somewhat diminished, as the affinity for TfnR for apo-Tfn is approximately tenfold less than for Fe_2Tfn.[21,27]

SDS-PAGE and Western blot analysis of Qβ-Tfn conjugates: Qβ VLP samples **1** and **5a**,**b** were analyzed on denaturing 4–12% NuPage protein gels using 1× MES buffer (Invitrogen). The gel was observed under UV illumination to detect fluorescent dye-labeled bands before staining with Coomassie SimplyBlue™ SafeStain (Invitrogen). For Western blot analysis, after electrophoretic separation on the gel, the proteins were transferred to a nitrocellulose membrane (Millipore) by electrophoretic blotting. After blocking with dry milk (5% (*w*/*v*)) in TBS-T for 1 h, transferrin conjugation to Qβ was detected with HRP-conjugated mouse monoclonal anti-transferrin antibody (Abcam), diluted 1:5000 in TBS-T buffer. HRP detection of peroxide was performed with SuperSignal chemiluminiscence substrate (Pierce) and exposure to X-ray film.

Cell culture and uptake studies: BSC1 monkey kidney epithelial cells stably expressing rat brain EGFP-clathrin light chain (EGFP-LCa) were provided by Dr. T. Kirchhausen, Harvard Medical School and cultured in DMEM supplemented with fetal bovine serum (FBS; 10%) and G418 (500 μg mL^{-1}). For microscopy studies, cells were plated on glass coverslip at a density of 8.3×10^3 cells cm^{-2} overnight. Cells were washed twice in PBS, and VLPs diluted in PBS^{4+} (1 mM $CaCl_2$, 1 mM $MgCl_2$, 0.2% BSA (*w*/*v*), and 5 mM glucose) at a concentration of 0.6 μg mL^{-1}. The cells were either kept at 0 °C for binding or shifted to 37 °C for the desired amount of time. The cells were washed again twice in PBS, and then fixed in paraformaldehyde (4%) for 30 min at RT. The cells were visualized at 60× magnifications using an Olympus X71 epifluorescence

 © 2010 Wiley-VCH Verlag GmbH & Co. KGaA, Weinheim

microscope equipped with the appropriate filter sets and a CCD camera.

Measurement of virus binding by flow cytometry: BSC1 cells were cultured on 15 cm dishes to confluency, and then lifted from surface by treating the cells with PBS/5 mM EDTA for 15 min at RT. The cells were centrifuged at 250 *g* for 10 min and resuspended in PBS^{4+} (500 μL). VLPs were added to the cells suspensions at 1:200 or 1:500 dilution and aliquoted to different tubes for incubation at 37 °C water bath for various amount of time. Cells were washed twice in PBS supplemented with FBS (1%), HEPES (25 mM), and EDTA (1 mM). The pelleted cells were finally resuspended in PBS (200 μL) and then fixed by adding paraformaldehyde (200 μL, 4%) in PBS. Fixed cells were typically analyzed within 1 h on Vantage Diva cell sorter.

Electron micrographs were acquired by using a Tecnai F20 Twin transmission electron microscope operating at 120 kV, a nominal magnification of 80 000×, a pixel size of 0.105 nm at the specimen level, and a dose of ~20 e^{-} $Å^{-2}$. 348 images were automatically collected by the Leginon system[28] and recorded using a Tietz F415 4k×4k pixel CCD camera. Experimental data were processed using the Appion software package.[29] 3554 particles were manually selected and then filtered down to 2239 particles for the reconstruction. The 3D reconstruction was carried out using the EMAN reconstruction package.[30] A resolution of 17.4 Å was determined by even–odd Fourier Shell Correlation (FSC) at a cutoff of 0.5.

Acknowledgements

This work was supported by the NIH (CA112075), The Skaggs Institute for Chemical Biology, and Pfizer Global Research and Development. The authors would like to thank Dr. Malcolm R. Wood for guidance in acquiring TEM images, Erica Jacovetty for assistance with cryo-EM data collection, Cody Fine for assistance with flow cytometry, and Steven D. Brown for mCherry-bearing particles. Cryo-EM imaging was performed at the National Resource for Automated Molecular Microscopy, which is supported by the National Institutes of Health though the National Center for Research Resources' P41 program (RR17573).

Keywords: click chemistry · polyvalency · receptor-mediated endocytosis · transferrin · viruses

[1] H. A. Huebers, C. A. Finch, *Physiol. Rev.* **1987**, *67*, 520.
[2] G. J. Anderson, C. D. Vulpe, *Cell. Mol. Life Sci.* **2009**, *66*, 3241.
[3] E. Ryschich, G. Huszty, H. P. Knaebel, M. Hartel, M. W. Buechler, J. Schmidt, *Eur. J. Cancer* **2004**, *40*, 1418.
[4] a) T. R. Daniels, T. Delgado, G. Helguera, M. L. Penichet, *Clin. Immunol.* **2006**, *121*, 159; b) T. R. Daniels, T. Delgado, J. A. Rodriguez, G. Helguera, M. L. Penichet, *Clin. Immunol.* **2006**, *121*, 144.
[5] a) H. Li, Z. M. Qian, *Med. Res. Rev.* **2002**, *22*, 225; b) H. Li, H. Sun, Z. M. Qian, *Trends Pharmacol. Sci.* **2002**, *23*, 206; c) Z. M. Qian, H. Li, H. Sun, K. Ho, *Pharmacol. Rev.* **2002**, *54*, 561; d) A. Widera, F. Norouziyan, W. C. Shen, *Adv. Drug Delivery Rev.* **2003**, *55*, 1439.
[6] A. S. L. Derycke, A. Kamuhabwa, A. Gijsens, T. Roskams, D. de Vos, A. Kasran, J. Huwyler, L. Missiaen, P. A. M. de Witte, *J. Natl. Cancer Inst.* **2004**, *96*, 1620.
[7] P.-H. Yang, X. Sun, J.-F. Chiu, H. Sun, Q.-Y. He, *Bioconjugate Chem.* **2005**, *16*, 494.
[8] S. Sen Gupta, J. Kuzelka, P. Singh, W. G. Lewis, M. Manchester, M. G. Finn, *Bioconjugate Chem.* **2005**, *16*, 1572.
[9] Q. Wang, E. Kaltgrad, T. Lin, J. E. Johnson, M. G. Finn, *Chem. Biol.* **2002**, *9*, 805.
[10] a) E. Strable, M. G. Finn, *Curr. Top. Microbiol. Immunol.* **2009**, *327*, 1; b) D. E. Prasuhn Jr. , P. Singh, E. Strable, S. Brown, M. Manchester, M. G. Finn, *J. Am. Chem. Soc.* **2008**, *130*, 1328.
[11] a) G. T. Hermanson, *Bioconjugate Techniques*, 2nd ed., Academic Press, San Diego, **2008**; b) K. F. Geoghegan, J. G. Stroh, *Bioconjugate Chem.* **1992**, *3*, 138; c) R. J. Goodson, N. V. Katre, *Biotechnologia* **1990**, *8*, 343.
[12] a) S. Petren, O. Vesterberg, *Biochim. Biophys. Acta, Protein Struct. Mol. Enzymol.* **1989**, *994*, 161; b) S. Welch in *Transferrin: The Iron Carrier*, CRC, Boca Raton, **1992**, p. 253; The number of sialic acid groups on transferrin, as well as the total serum sialic acid level, is used as a diagnostic marker of alcoholism, see: c) L. Chrostek, B. Cylwik, A. Krawiec, W. Korcz, M. Szmitkowski, *Alcohol Alcohol.* **2007**, *42*, 588–592.
[13] Y. Beguin, G. Bergamaschi, H. A. Huebers, C. A. Finch, *Am. J. Hematol.* **1988**, *29*, 204.
[14] a) Y. Cheng, O. Zak, P. Aisen, S. C. Harrison, T. Walz, *J. Struct. Biol.* **2005**, *152*, 204; b) Y. Cheng, O. Zak, P. Aisen, S. C. Harrison, T. Walz, *Cell* **2004**, *116*, 565.
[15] a) P. E. Dawson, S. B. H. Kent, *Annu. Rev. Biochem.* **2000**, *69*, 923; b) A. Dirksen, T. M. Hackeng, P. E. Dawson, *Angew. Chem.* **2006**, *118*, 7743; *Angew. Chem. Int. Ed.* **2006**, *45*, 7581.
[16] V. Hong, S. I. Presolski, C. Ma, M. G. Finn, *Angew. Chem.* **2009**, *121*, 10063; *Angew. Chem. Int. Ed.* **2009**, *48*, 9879.
[17] S. D. Brown, J. D. Fiedler, M. G. Finn, *Biochemistry* **2009**, *48*, 11155.
[18] R. A. Warren, F. A. Green, C. A. Enns, *J. Biol. Chem.* **1997**, *272*, 2116.
[19] D. Loerke, M. Mettlen, D. Yarar, D. Jaqaman, H. Jaqaman, G. Danuser, S. L. Schmid, *PLoS Biol.* **2009**, *7*, e57.
[20] H. M. Van der Schaar, M. J. Rust, C. Chen, H. Van der Ende-Metselaar, J. Wilschut, X. Zhuang, *PLoS Pathog.* **2008**, *4*, e1000244.
[21] A. Ciechanover, A. L. Schwartz, A. Dautryvarsat, H. F. Lodish, *J. Biol. Chem.* **1983**, *258*, 9681.
[22] For definitions and discussion of affinity and avidity in the context of polyvalent interactions, see: M. Mammen, S.-K. Choi, G. M. Whitesides, *Angew. Chem.* **1998**, *110*, 2908–2953; *Angew. Chem. Int. Ed.* **1998**, *37*, 2754–2794. We also recommend the following paper for an excellent example of their application: E. Arranz-Plaza, A. S. Tracy, A. Siriwardena, J. M. Pierce, G.-J. Boons, *J. Am. Chem. Soc.* **2002**, *124*, 13035–13046.
[23] E. W. Marsh, P. L. Leopold, N. L. Jones, F. R. Maxfield, *J. Cell Biol.* **1995**, *129*, 1509.
[24] C. J. Lim, W. C. Shen, *Pharm. Res.* **2004**, *21*, 1985.
[25] M. W. Goldberg, H. H. Lehr, M. Muller, (Hoffmann-–La Roche), US patent 3398180, **1968**.
[26] O. Zak, K. Ikuta, P. Aisen, *Biochemistry* **2002**, *41*, 7416.
[27] a) A. Dautry-Varsat, A. Ciechanover, H. F. Lodish, *Proc. Natl. Acad. Sci. USA* **1983**, *80*, 2258; b) T. Hasegawa, E. Ozawa, *Devel. Growth Differ.* **1982**, *24*, 581.
[28] C. Suloway, J. Pulokas, D. Fellmann, A. Cheng, F. Guerra, J. Quispe, S. Stagg, C. S. Potter, B. Carragher, *J. Struct. Biol.* **2005**, *151*, 41.
[29] a) G. C. Lander, S. M. Stagg, N. R. Voss, A. Cheng, D. Fellmann, J. Pulokas, C. Yoshioka, C. Irving, A. Mulder, P.-W. Lau, D. Lyumkis, C. S. Potter, B. Carragher, *J. Struct. Biol.* **2009**, *166*, 95; b) N. R. Voss, D. Lyumkis, A. Cheng, P.-W. Lau, A. Mulder, G. C. Lander, E. J. Brignole, D. Fellmann, C. Irving, E. L. Jacovetty, A. Leung, J. Pulokas, J. D. Quispe, H. Winkler, C. Yoshioka, B. Carragher, C. S. Potter, *J. Struct. Biol.* **2010**, *169*, 389.
[30] S. J. Ludtke, P. R. Baldwin, W. Chiu, *J. Struct. Biol.* **1999**, *128*, 82.

Received: February 26, 2010
Published online on May 7, 2010

 © 2010 Wiley-VCH Verlag GmbH & Co. KGaA, Weinheim